Studies of Low-Frequency Molecular Motions in Polymers by Neutron Inelastic Scattering

S. Trevino[ab]; H. Boutin[ab]

[a] PICATINNY ARSENAL, DOVER, NEW JERSEY [b] Presently guests at Army Materials Research Agency, Watertown, Mass

PLEASE SCROLL DOWN FOR ARTICLE

Studies of Low-Frequency Molecular Motions in Polymers by Neutron Inelastic Scattering

S. TREVINO* and H. BOUTIN*

PICATINNY ARSENAL
DOVER, NEW JERSEY

Summary

The energy distribution of a monoenergetic incident neutron beam after a single scattering event provides information concerning the molecular motions of a polymer in the region 800 to 30 cm⁻¹. In polyethylene (Marlex 6050) several peaks are observed in the neutron spectrum between 200 and 600 cm⁻¹. The frequencies corresponding to these peaks are in good agreement with those predicted from a calculation of the dispersion relations of the skeletal modes (bending and stretching) taking into account interchain forces. In the case of an oriented sample of the polymer, a polarization effect can be obtained by placing the momentum transfer $\bar{K}$ of the neutron parallel or perpendicular to the chain direction $\bar{S}$. This allows the identification of transverse and longitudinal modes of vibration. This effect has been studied in the case of polyethylene and polyoxymethylene. The frequency distribution of phonons, derived from the neutron data under certain approximations, were also obtained from samples of polyoxymethylene, polyacrylonitrile, and polyethylene glycol. These results are compared with the observed infrared and the calculated frequencies.

INTRODUCTION

The technique of inelastic neutron scattering has been applied to the study of the low-frequency motions in polymers (1–7). These studies have lead to the tentative assignment of frequencies to the various characteristic vibrations of the chain. These assignments have been made on the basis of comparison with observed infrared adsorption frequencies, Raman spectra, and various normal mode calculations. The polymer most intensively studied with this tech-

* Presently guests at Army Materials Research Agency, Watertown, Mass.

nique has been polyethylene (PE) (2-7). The simplicity of its struc-
ture, transplanar, and the fact that the chemical unit (CH_2) contains
three atoms, leads to a relatively small number (9) of normal modes
for the chain. PE is also the only polymer for which a complete
normal-mode calculation of the nonfactor group frequencies as a
function of δ (phase difference between two adjacent CH_2 units)
has thus far been performed (8,9). These calculations can be used
to derive the frequency distribution of the lattice, which can in
turn be compared with the frequency distribution derived through
an approximation from the neutron scattering data. The possibility
of using the neutron measurements to verify the results of the cal-
culations of the various modes which are in a frequency range un-
attainable at the present time by optical techniques or which are
optically inactive, together with the questions which have arisen
as to the validity of such calculations, make the technique of neu-
tron inelastic scattering a useful and promising tool in molecular
spectroscopy.

NEUTRON SCATTERING THEORY

The relationship between the vibrational motions of the sample
and the scattering cross section of neutrons has been investigated
quite extensively (10). The inelastic scattering of neutrons is the
process in which the energy of the neutron is altered due to an ab-
sorption or emission of one or more phonons. One can further clas-
sify the scattering into coherent and incoherent scattering. Co-
herent scattering is that type which exhibits interference effects
analogous to the diffraction of light. Not all nuclei scatter neutrons
coherently and, in particular, the hydrogen nucleus scatters neu-
trons almost completely incoherently. In addition, the scattering
cross section of hydrogen (81.5 barns) is much larger than that of
carbon (5.5 barns). It is, therefore, a good approximation to say that
hydrogenous polymers scatter neutrons via the hydrogen nuclei
and incoherently. We will therefore limit our attention to the in-
elastic incoherent scattering of neutrons.

The cross section can be expanded into a series of terms ex-
pressing the probabilities for absorption (or emission) of one or
several phonons:

$$d^2\sigma/d\Omega\ dE = \sum_l d^2\sigma(l)/d\Omega\ dE \qquad (1)$$

where l is the number of phonons involved in the interaction. The largest contribution to scattering is from the single phonon ($l = 1$) term with each successive term diminishing in magnitude.

Now, in general, the motion of the various nuclei in a crystal can be treated as a superposition of plane waves (phonon) characterized by their wave vector $\bar{q}$, frequency $\omega_j(\bar{q})$, and polarization vector $\bar{C}_j^k(\bar{q})$. The subscript j refers to the jth branch of normal modes and k to the kth nucleus in the unit cell. The vibrational properties of a crystal can also exhibit themselves in terms of the vibrational frequency distribution $g(\omega)$, which expresses the density of eigenstates as a function of frequency. The relationship between $g(\omega)$, ω, and $\bar{q}$ is given by

$$g(\omega) = (V_0/N) \sum_j \int (dS/|\nabla_{\bar{q}} \omega_j(\bar{q})|)$$

where V_0 is the volume of the unit cell and N the number of nuclei in the unit cell. The integration is carried out over surfaces of constant ω. The thermodynamic properties of a crystal can be calculated from the frequency distribution, so this function is of considerable importance.

In general, the neutron scattering cross section is not expressable in terms of $g(\omega)$ but rather must be expressed as a function ω_j, $\bar{q}$, and $\bar{C}_j^k$. The expression for the one-phonon absorption cross section has been derived by Sjölander (10) to be

$$\frac{d^2\sigma^{(1)}}{d\Omega \, d\omega} = \sum_n A_n \frac{k_f}{k_0} e^{-2W_n} \frac{\hbar^2 K^2}{2M_n} \frac{1}{N} \sum_j \frac{\coth(\beta\omega_j) + 1}{2\omega_j}$$

$$|\bar{e}_K \cdot \bar{C}_j^n|^2 \, \delta(\omega_f - \omega_0 + \omega_j) \quad (2)$$

$$\bar{K} = \bar{k}_f - \bar{k}_0$$

where A_n is the scattering cross section of the nth nucleus in the unit cell, k_0 and k_f are the wave vectors of the incident and scattered neutrons, M_n the mass of the nth nucleus, $\beta = \hbar/k_B T$, and $\bar{e}_k$ is a unit vector in the direction of $\bar{K}$. The term e^{-2W_n} is the well-known Debye-Waller factor and is given by

$$2W_n = \frac{\hbar^2 K^2}{2M_n} \frac{1}{N} \sum_j \omega_j^{-1} \coth(\beta\omega_j) |\bar{e}_K \cdot \bar{C}_j^n|^2 \quad (3)$$

As can be seen from the above equations, an exact calculation of the scattering cross section would require a knowledge not only of the eigenfrequencies ω_j but also of the eigenvectors $\bar{C}_j^n$. For a simple crystal this calculation is difficult, and it becomes quite cumbersome for a molecule like polyethylene.

Under certain conditions it can be shown that a simpler equation for the cross section constitutes a valid approximation. Tarasov (11) has shown that a polycrystalline sample which is isotropic has approximately the same scattering characteristics as a cubic lattice. These changes in Eq. (2) would consist of averaging over crystal orientation and setting

$$\sum_j \bar{C}_{jx}^n \cdot \bar{C}_{jy}^n = \delta_{xy} \tag{4}$$

The result of these approximations is

$$\frac{d^2\sigma^{(1)}}{d\Omega\,d\omega} = A\,\frac{k_f}{k_0}\,e^{-2W}\,\frac{\hbar^2 K^2}{2M}\,\frac{g(\omega)}{\omega}\,\frac{\delta(\omega_j - \omega_0 + \omega)}{(e^{\beta\omega} - 1)} \tag{5}$$

where here $M = \sum_n M_n$, the mass of the unit cell.

Equation (5) relates the scattering cross section to the frequency distribution function $g(\omega)$ directly. This is a considerably simpler expression than Eq. (2). The expressions for W_n and the cross section for two phonon processes can also be derived more simply using this approximation.

The general feature of the neutron scattering technique can be seen by inspection of Eq. (5), the most notable being that for isotropic polycrystalline samples there exist no selection rules to limit the observation of vibrations. However, if the sample has some preferred orientation, the term $|\bar{e}_K \cdot \bar{C}_j^n|^2$ in Eq. (2) will influence the heights of the various peaks which correspond to motion along different directions in the crystal.

Experimental Technique

The instrument used in the present study is a conventional time-of-flight spectrometer. It has been described in detail in the literature (2). For completeness, a short description of the spectrometer will be given here. Figure 1 is a schematic drawing of the instrument. The beam of neutrons from the core of the U.S. Army Materials Research reactor (1 MW light-water-moderated) is passed

DETECTORS

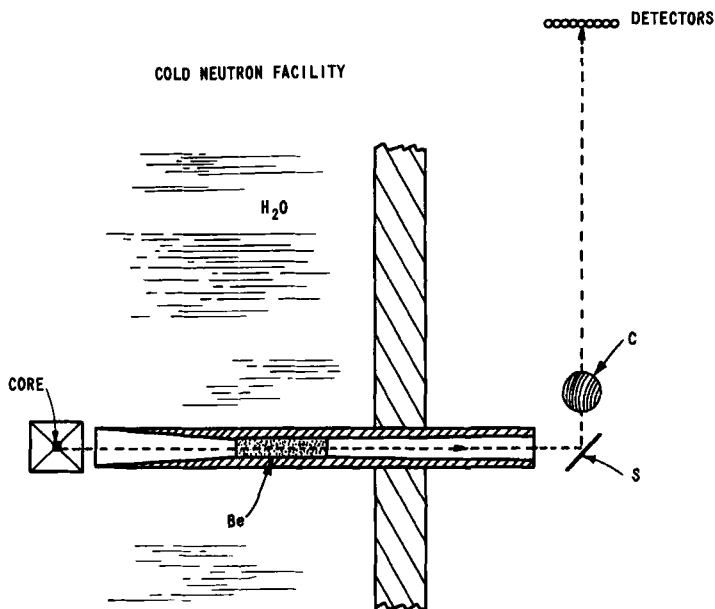COLD NEUTRON FACILITY

H_2O

C

CORE

Be

S

FIG. 1. Schematic drawing of the time-of-flight spectrometer.

through a 16-inch sample of polycrystalline beryllium. The Be acts as a low-pass filter, allowing only those neutrons whose energy is less than 0.0052 eV (42 cm^{-1}) to be transmitted. This quasi-mono-chromatic beam impinges upon the sample S. The neutrons scattered by the sample through an angle of 90° are energy-analyzed by measuring their flight time across a fixed distance (5 m). This is accomplished by "chopping" the beam with a set of rotating slits C, which provide an initial time from which to measure the flight time to the detector. The spectrum is recorded by a 256-channel analyzer whose channel width is 32 μsec.

Polyethylene

The vibrational modes of the polyethylene chain have been extensively investigated by various techniques. Infrared and Raman spectra have been used to identify the high-frequency motions (>700 cm^{-1}), and normal coordinate calculations have been successful in reproducing the observed frequencies (8). These calculations have led to a reliable set of force constants for the extended

chain. Only the very low frequency chain modes (<600 cm^{-1}) have not been susceptible to investigation by optical techniques. The selection rules which govern the interaction of light with solids forbids direct observance of some of these frequencies. It should be pointed out that the selection rules are symmetry-dependent. A lifting of the symmetry by allowing the polymer to take on conformations other than the transplanar would make some frequencies active. This indeed has been observed for polyethylene in which broad bands centered at 600 and 200 cm^{-1} have been observed (*12*).

The neutron scattering technique has been applied to the study of these modes (*2–7*). In all the work done to date, the spectra have been analyzed using Eq. (5). The frequency distribution of Danner et al. (*2*) is reproduced in Fig. 2. This function was derived from a spectrum obtained with a time-of-flight spectrometer, of a high-density sample of Marlex 6050 held at liquid-nitrogen temperature. The high-frequency limits of the two modes ν_5 and ν_9 (*8*) were taken at 520 ± 15 and 190 ± 10 cm^{-1}, respectively, corresponding to the peaks shown in Fig. 2. Subsequent measurements using both time-of-flight techniques and a triple crystal spectrometer have confirmed the existence of these peaks in the neutron spectra. The assignments of the remaining peaks in the spectra have been more tentative.

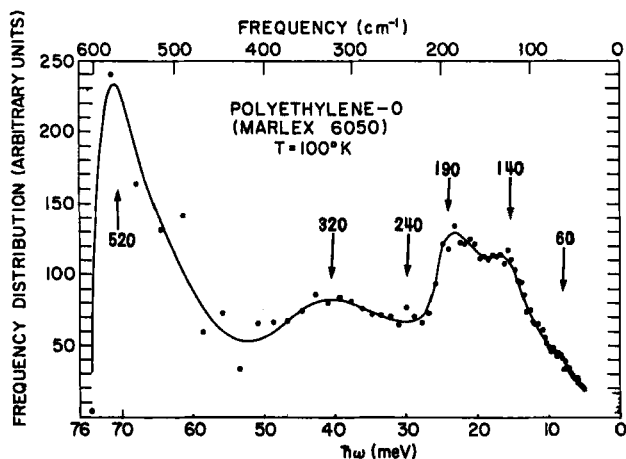Recently, Myers et al. (*7*) have performed measurements on a

FIG. 2. Frequency distribution of polyethylene derived by Danner et al. (*2*). The vibrational frequencies are indicated in cm^{-1}.
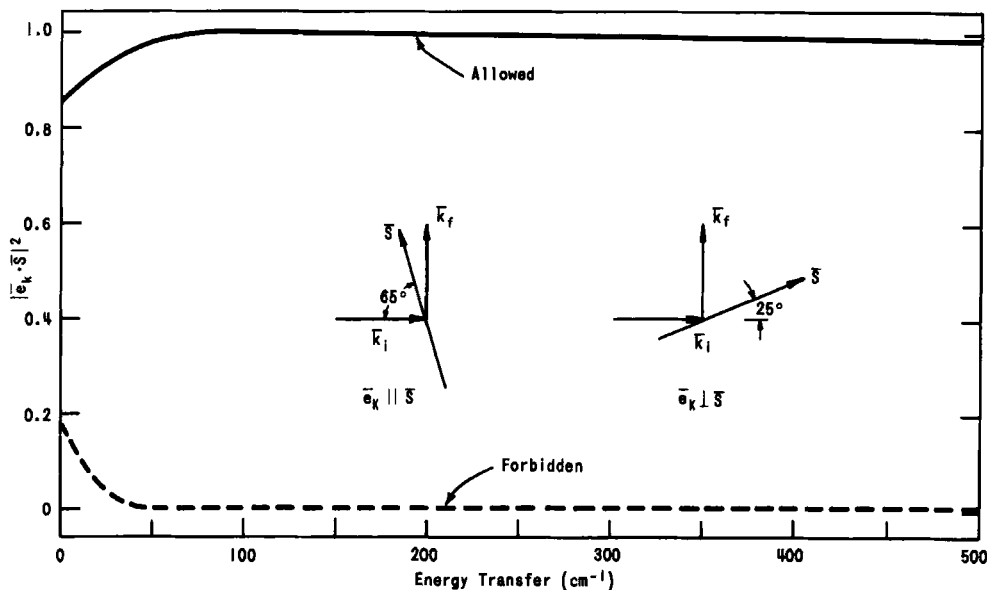
FIG. 3. Schematic drawing of the sample orientation used in the present measurement. $\bar{k}_i$ and $\bar{k}_f$ and $\bar{S}$ are, respectively, the wave vectors of the incident and final neutrons and the orientation direction of the sample. The function $|\bar{e}_K S|^2$ is plotted as a function of energy transfer in cm^{-1}.

stretch-oriented sample of the polymer. The experiment was designed to test the effect of the term $|\bar{e}_K \cdot \bar{C}_j^n(\bar{q})|^2$ in Eq. (2). The momentum transfer K was placed alternately parallel and perpendicular to the chain direction. Vibrational modes for which the hydrogen atoms move perpendicular to the chain (ν_9) would not contribute to the scattering when $\bar{e}_K$ is parallel to the chain. Similarly, ν_5 should not contribute to the scattering when $\bar{e}_K$ is perpendicular to the chain axis. The peak at 520 cm^{-1} was shown to be a longitudinal mode and its assignment to ν_5 was confirmed. The peak at 190 cm^{-1} was, however, not completely eliminated when $\bar{e}_K$ was placed parallel to the chain. This threw some doubt on the assignment of this to ν_9. The measurement of neutron scattering from an oriented sample of polyethylene was repeated using the time-of-flight spectrometer. The sample of the polymer was oriented by stretching and rolling.* X-ray diffraction measurements show that

* The sample was provided by Dr. H. Starkweather of E. I. du Pont de Nemours & Co.

the polymer chains are aligned parallel to the long direction of the sample with a distribution characterized by an angular width of about 4.7° at half-maximum. Although it is not possible to place $\bar{e}_K$ exactly parallel (or perpendicular) to the chain axis for all values of energy transfer, a satisfactory effect can be obtained with but one orientation. The orientation which was used is drawn schematically in Fig. 3. The function $|\bar{e}_K \cdot \bar{S}|^2$ is given in this figure as a function of energy transfer for the two cases in which transitions are allowed or forbidden according to whether the polarization vectors are parallel or perpendicular to $\bar{K}$, respectively. As can be seen from the figure, the effective selection rules are operative to a satisfactory degree. The results of the measurement in which the sample temperature was 293°K are shown in Fig. 4. The time-of-flight spectrum is plotted as a function of energy transfer in cm^{-1}. The general features of the spectra confirm the results of Myers et al. The mode ν_5 is clearly identified. Again, the peak at 190 cm^{-1} is not completely eliminated by placing $\bar{e}_K$ parallel to the chain. However, there is a definite peak at 240 cm^{-1} in the perpendicular measurement which seems to be eliminated in the parallel one. It is therefore suggested that this peak at 240 cm^{-1} be assigned to ν_9. This is in agreement
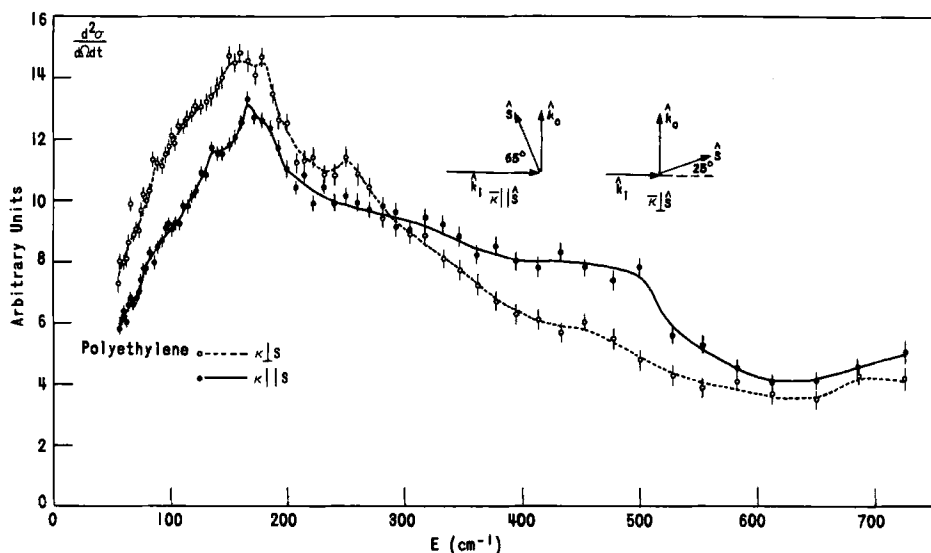

FIG. 4. Results of the measurements on the oriented sample of PE. The time-of-flight spectrum is plotted as a function of energy transfer in cm^{-1}.
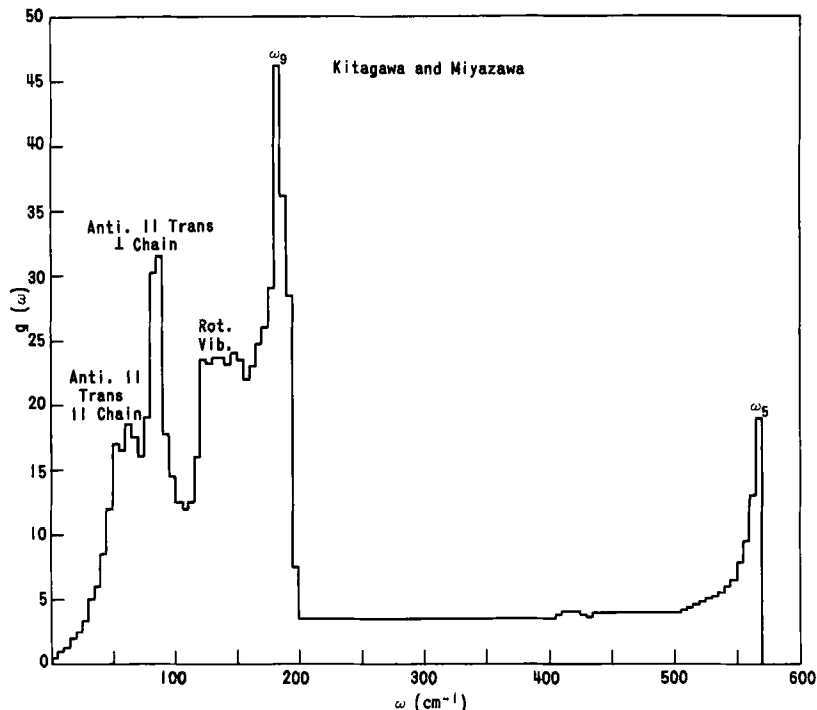
FIG. 5. Frequency distribution of PE as calculated by Kitagawa and Miyazawa (9).

with a recent calculation by Tasumi and Shimanouchi (8) of the frequency vs. phase curves for an extended polyethylene chain in the crystalline field of its neighbors. This calculation shows the effect of the crystalline field on the chain modes and in particular predicts the splitting of ν_9 into two rather well separated branches. The high-frequency limits of the two branches are given as 240 and 225 cm^{-1} On the other hand, Kitagawa and Miyazawa (9) have also performed such a calculation. The frequency distribution they obtained is reproduced in Fig. 5. The high-frequency limits of ν_5 and ν_9 are given as 570 and 200 cm^{-1} and no splitting is shown for ν_9. This discrepancy in the two calculations seems to be due to the values of the crystalline force constants used by the different authors, the former author using a substantially stronger field. The present measurement seems to favor the results of Tasumi and

Shimanouchi, although the observation of the splitting of ν_9 is not apparent. This may be due in part to the resolution of the instrument used in the present measurement.

In addition to the frequencies due to the chain modes, three additional peaks are predicted, as shown in Fig. 5. The broad peak at 140 cm^{-1} is due to over-all rotatory vibration of the chains about the axis. The peak at 90 cm^{-1} is due to antiparallel translatory vibrations of adjacent chains perpendicular to the chain axis, and the peak near 60 cm^{-1} is due to antiparallel translatory vibrations parallel to the chain axis. The time-of-flight spectrum obtained by Danner et al. shows a peak at 240 cm^{-1} for which no interpretation was provided. If we assign this peak to ν_9, there are three peaks below ν_9 which could be assigned to the three lattice peaks of Kitagawa and Miyazawa. The resolution of the spectrometer, which is a function of neutron energy, becomes rather poor for energy transfer above about 200 cm^{-1}. To obtain a more accurate value of $g(\omega)$, these resolution effects should be removed if possible from the data. In the present work, the time-of-flight spectrum is calculated from $g(\omega)$ in the one-phonon approximation using Eq. (5), and the spectrum is broadened according to a Gaussian shape. In this manner, the data of Danner et al. is reproduced from the empirically con-
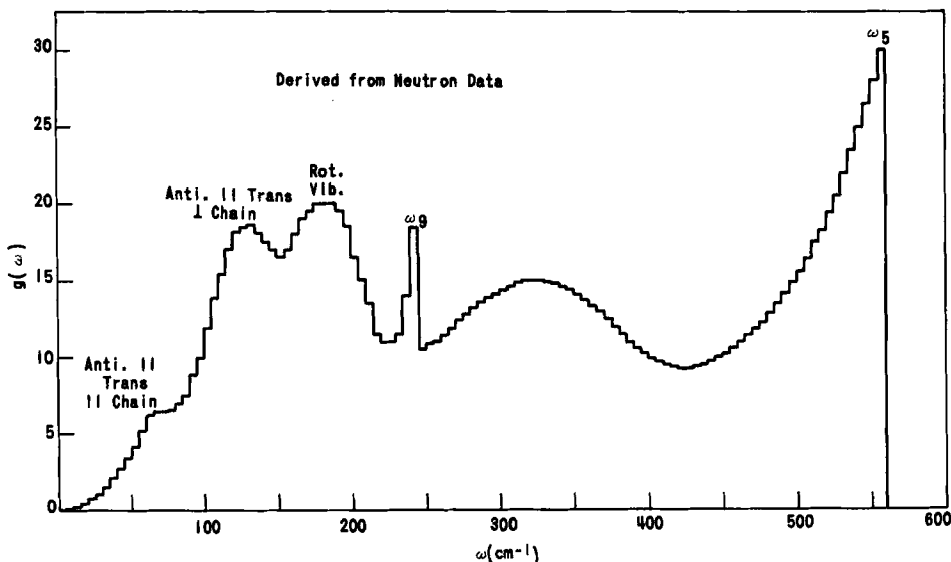

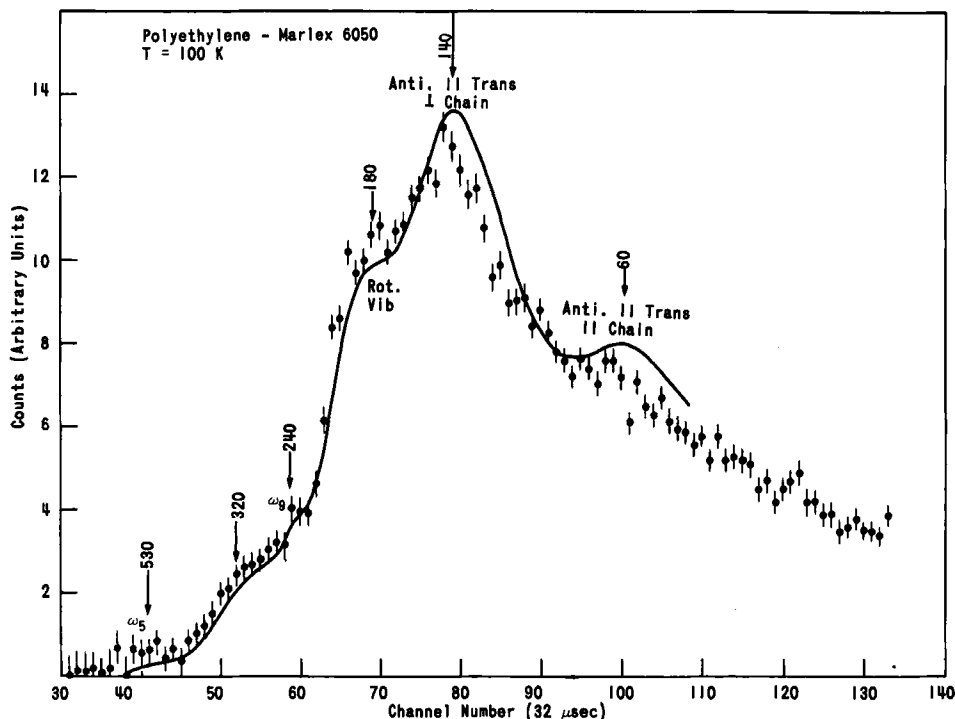FIG. 6. Frequency distribution used to fit the data of Danner et al. (2).

FIG. 7. Time-of-flight distribution of neutrons scattered at $T = 100°K$ by a sample of PE (Marlex 6050). The solid line is the result of the calculation in which instrumental resolution and incident line shape are taken into account in reproducing the data.

structed frequency distribution shown in Fig. 6. The results of this calculation are shown as the solid line of Fig. 7, where the points are the observed spectrum. It can be seen that a peak is required in $g(\omega)$ at 240 cm^{-1} to reproduce the corresponding structure in the spectrum. Table 1 shows a comparison between the calculations of Tasumi and Shimanouchi and Kitagawa and Miyazawa, and the present assignments. The observed frequencies of the lattice modes are generally higher than those of the calculations. The calculations were performed for a room-temperature sample while the experiment was performed at 100°K. The observed frequencies are thus expected to be higher.

There is another feature of the frequency distribution proposed in the present work which must be explained. This is the discrep-

TABLE 1

Comparison of the Vibrational Frequencies Obtained by Neutron Scattering Measurements with the Results of Calculations by Tasumi and Shimanouchi and Kitagawa and Miyazawa

Neutron	Tasumi and Shimanouchi	Kitakawa and Miyazawa	Assignment
520	520	510	ν_5
320			
240	240	200	ν_9^a
190 (broad)	225	140	Rotatory vibrations
	160		
140 (broad)	100	90	Translation $\perp$ axis
60 (broad)	70	60	Translation $\parallel$ axis

ancy in the relative sizes of the observed peaks corresponding to the various motions. It will be noted that the peak corresponding to ν_5 is larger than that due to ν_9, whereas the calculations of $g(\omega)$ shows just the opposite effect. Also, the size of the peaks due to rotatory motions and translation perpendicular to the chain axis are much larger than that due to translation along the chain. This raises the question of the accuracy of the proposed frequency distribution in reflecting the relative heights of the various peaks. The additional broad band centered at 325 cm^{-1} falls in the same category. There are several possible explanations:

1. The sample of polyethylene used in this measurement was high-density Marlex 6050. The sample certainly contained regions of disorder and defects. The influence of these regions on the motions of the ideal extended chain in the well-ordered crystalline field of its neighbors could possibly give rise to some of these discrepancies. The spectrum obtained from a sample of polyethylene crystals grown from solution also exhibits the broad band at 325 cm^{-1} (5). This measurement would suggest that the amorphous regions are not responsible for this band, but since the sample consists of folded chains, the influence of fold defects cannot be eliminated.

2. These peaks could also correspond to combinations or multiple scattering, which can be observed in the neutron spectra although they are expected to be very weak.

3. Possibly the more reasonable explanation is that the approxi-

mate expression [Eq. (5)] used to obtain $g(\omega)$ from the data con-
stitutes a rather poor approximation. The effect of the amplitude
of vibration on the cross section might produce this discrepancy in
the relative heights of the observed structure. Only an exact calcu-
lation of the cross section can detect the size of this effect.

The specific heat of crystalline polyethylene has been obtained
by Wunderlich (13). The calculation of this quantity from any
proposed frequency distribution should constitute a test of its
validity. Kitagawa and Miyazawa calculated the specific heat up to
150°K using their frequency distribution and obtained quite a good
fit. In the present work, the specific heat has been calculated using
the frequency distribution of Fig. 6. The results are shown in Fig. 9.
As can be seen, the agreement is rather poor. A second calculation
is performed using a frequency distribution obtained in the follow-
ing manner. The relative height of the various peaks are chosen to
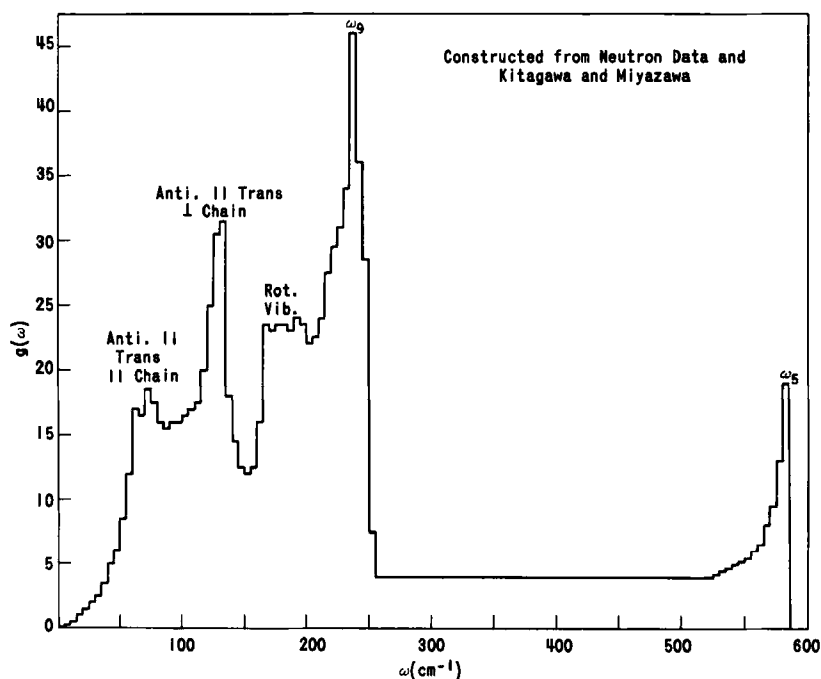conform with the calculation of Kitagawa and Miyazawa but their

FIG. 8. Frequency distribution of polyethylene constructed as described in
the text.
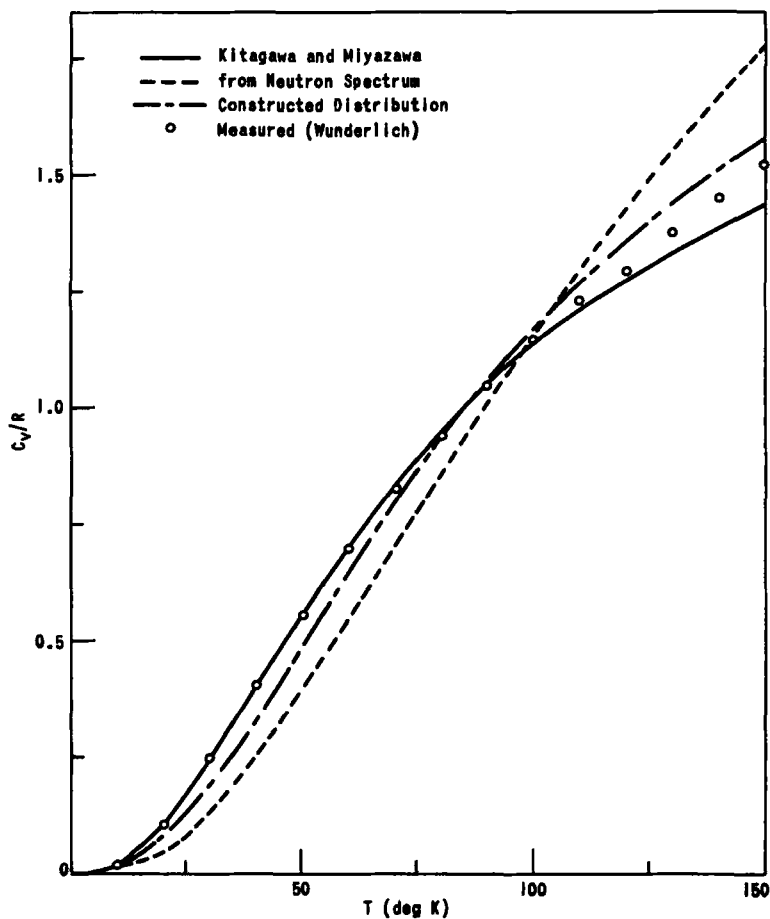
FIG. 9. Comparison of the measured specific heat of polyethylene with various calculations.

energies are chosen from the neutron scattering data. This yields a frequency distribution shown in Fig. 8 and a calculated specific heat in Fig. 9. The agreement is much better in the latter case. The specific heat obtained by Kitagawa and Miyazawa is also shown for comparison.

In summary, there is some evidence from the measurements on the oriented sample of polyethylene that the high-frequency limit of ν_9 could occur at 240 cm^{-1} and the three peaks below this would

then be assigned to the lattice modes. These frequencies agree with those predicted by the latest calculation of Tasumi and Shimanouchi.

Polyethyleneoxide

The helical structure of polyethyleneoxide (PEO) has been well established as containing seven chemical units (CH_2—CH_2—O) and two turns in the fiber identity period (*14*). Infrared and Raman data have been analyzed using this conformation and good agreement has been obtained (*14*; see Table 2). The number of frequencies given in these calculations, although small, are sufficient to identify the majority of the peaks observed in the neutron spectrum. Figure 10 shows the frequency distribution of a sample of PEO (Carbowax, average molecular weight 20,000) at 293°K derived from the neutron spectrum. A second sample with a different molecular-weight distribution (Carbowax 6000) was also studied and some small differences were observed between the two spectra. OCC and COC bending combine out of phase to give the peaks at

TABLE 2

Comparison of Vibrational Frequencies in PEO Observed by Raman, Infrared, and Neutron Measurements with the Calculated Values[a]

IR	Raman	Calc.	Neutrons	Assignments[b]
1060		1041		
		954		$\nu(CC)(58) + \nu(CH)_i(25)$
	860	876		$r(CH_2)_i(53) - \nu(CO)_i(32)$
	845	856	868	$r(CH_2)_o(79)$
532		530	535	$\delta(OCC)_o(96)$
530	531	494		$\delta(OCC)_o(65) + \delta(OCC)_i(15)$
	360	366		$\delta(COC)(43) + \delta(OCC)_i(23)$
		350	310–380	
	275	270		$\delta(OCC)_i(25) + \delta(COC)(21) - \tau(CC)(14)$
215		221	228	$\delta(COC)(47) + \tau(CC)(26) + \delta(OCC)_o(16)$
165		162		$\tau(CC)(33) + \tau(CO)_o(25) + \delta(OCC)_i(22)$
106		116	120	$\tau(CO)_o(100)$
		100		$\tau(CO)_i(80)$
			80	
			51	

[a] The possible assignments are taken from Tadokoro et al. (*14*).
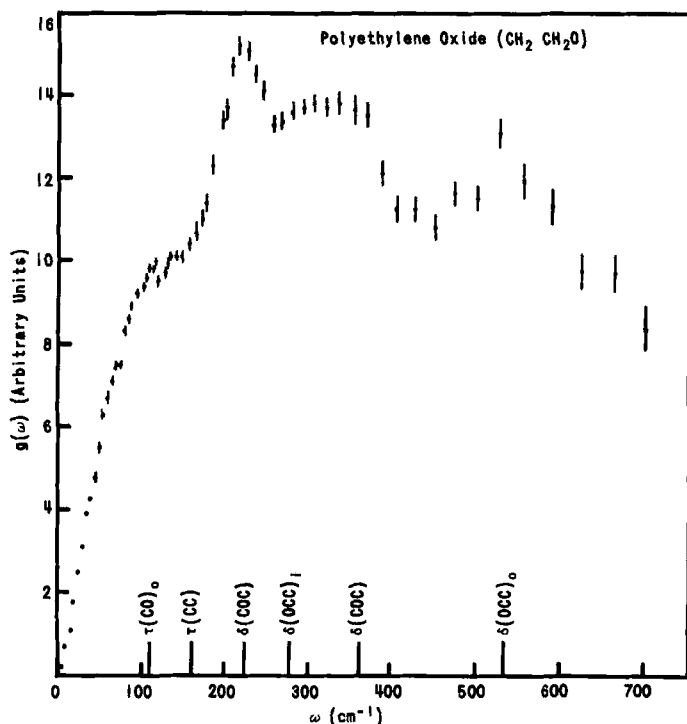[b] τ, torsion; δ, bending; ν, stretching; r, rocking.

FIG. 10. Frequency distribution derived from the neutron data for a sample of polyethyleneoxide (Carbowax average molecular weight 20,000). The observed infrared frequencies are indicated together with their assignment.

535 cm^{-1} and in phase to give the broad band centered at 310 cm^{-1}. The broad region below 200 cm^{-1} is likely to contain a rather complicated combination of torsion and possibly some lattice vibrations, although these probably lie below 100 cm^{-1}. A more definite assignment of the various structure visible in the frequency distribution will be attempted upon completion of the normal coordinate calculations in progress at the present time.

Polyacrylonitrile

The conformation and tactic structure of polyacrylonitrile (PAN) have not been unambiguously determined because of the generally diffuse X-ray diffraction patterns. Bohn et al. (*15*) have interpreted

this result as indicating the existence of no valid repeat distance along the chain. There is general agreement about a lateral packing of cylinders within which the chain exists but no evidence that the chains assume any specific structure in these cylinders. Treatment of the sample with heat changes the lateral order from hexagonal to orthorhombic. There are at least two reported transition temperatures in PAN at 87 and 140°C. Andrews and Kimmel (16) have studied the 140°C transition with birefrigerance and show that an irreversible ordering occurs when the polymer is heated above this temperature and allowed to cool. These results are interpreted by these authors as due to the loosening and reformation of a dipole association structure. Bohn et al. have also noted this ordering upon heating from the X-ray measurements. There is, however, no reported increase in the longitudinal order upon heating.

The infrared spectra of PAN have been obtained by several investigators (17,18) and have analyzed with some degree of success using a transplanar model for the chain. There are differences in the observed frequencies and, since different tactic structures were assumed, differences in the assignments of various bands. Yamadera et al. (18) conclude from the results of infrared and normal coordinate calculation that it may be possible that PAN contains a structure very close to the syndiotactic planar zigzag but that enough discrepancies exist so that deviation from this structure cannot be eliminated (see Table 3).

In the present work the spectra of neutrons inelastically scattered from two samples of PAN have been obtained. Sample 1* is in the form of a fine-grain powder. The X-ray diffraction pattern of this sample shows a large, rather sharp reflection corresponding to a spacing of about 5.2 Å and a weaker reflection corresponding to a spacing of approximately 3 Å. There is a general diffuse scattering covering a large portion of the pattern. Sample II† is a film cast from solution (H_2O and NaSCN). The X-ray pattern of this sample again shows the 5.2-Å reflection but it is considerably weaker and much broader. The 3-Å reflection is almost completely lost in the greatly increased diffuse scattering. Upon heating above 150°C, however, the X-ray spectrum of sample II sharpens and becomes similar to that of sample I. The frequency distributions derived

* Provided by Dr. H. Starkweather of E. I. du Pont de Nemours & Co.
† Provided by Dr. J. Powers of American Cyanamid Co.

TABLE 3

Comparison of Vibrational Frequencies in PAN Observed by Infrared and
Neutron Measurements with Calculated Values[a]

Neutrons	Infrared	Calc.	Assignment[b]
1210 (broad)	1247 ($\parallel$)	1189	$\omega(CH)(40) + \omega(CH_2)(29) - \nu_a(CC)(26)$
	1115 ($\perp$)	1101	$\nu_s(CC)(33) - \delta(CH)(20)$
	1073 ($\perp$)	1080	$\nu_s(CC)(69)$
		1060	$r(CH)(47) - \delta(C-C-CN)(21)$
	1015 ($\parallel$)	1018	$\omega(CH)(57) + \nu_a(CC)(26)$
		999	$. t(CH)(59)$
800 (broad)	865 ($\parallel$)	847	$r(CH)(91)$
	778 ($\perp$)	796	$\nu(C-CN)(48) + t(CH_2)(34)$
		764	$\nu(C-CN)(59) - r(CH_2)(28)$
565	570 ($\perp$)	551	$\delta(C-C-CN)(53) - \delta(C-C-N)(22)$
	537 ($\perp$)	518	$\delta(C-C-CN)(34) - \delta(C-C-N)(37)$
	520 (no)	524	$\omega(C-C-CN)(45) - \omega(C-C-N)(40)$
380			
338		357	$\delta(C-C-C)(65)$
280	260 ($\perp$)	271	$\delta(C-C-N)(58) + \delta(C-C-CN)(19)$ $- \delta(C-C-C)(19)$
		246	$\delta(C-C-N)(63) + \delta(C-C-CN)(28)$
170		204	$\omega(C-C-N)54 + \omega(C-C-CN)(40)$
85			
50			

[a] The possible assignments are taken from the paper of Yamadera et al. and Miyazawa (18). The frequencies are expressed in cm^{-1}.

[b] ν, stretching; ν_s, symmetric stretching. ν_a, antisymmetric stretching. δ, bending; ω, wagging; r, rocking; t, twisting.

from the neutron measurements are shown in Fig. 11. The peaks centered at 560 and 265 cm^{-1} agree with infrared lines observed in these energy regions and can be assigned to low-lying optical modes (bending or wagging). The $g(\omega)$ displays a minimum at $\omega = 430$ cm^{-1}, where an infrared line has been reported (17). These two observations, however, are not necessarily in disagreement. Some of the optically active modes need not occur in regions where there exist a large density of states. The broad shoulder extending from approximately 50 to 160 cm^{-1} covers the frequency range in which the low-energy acoustic modes are expected. Any specific structure in this part of the spectrum is taken as an indication of the degree of order along the chain, as these low-energy acoustic modes are
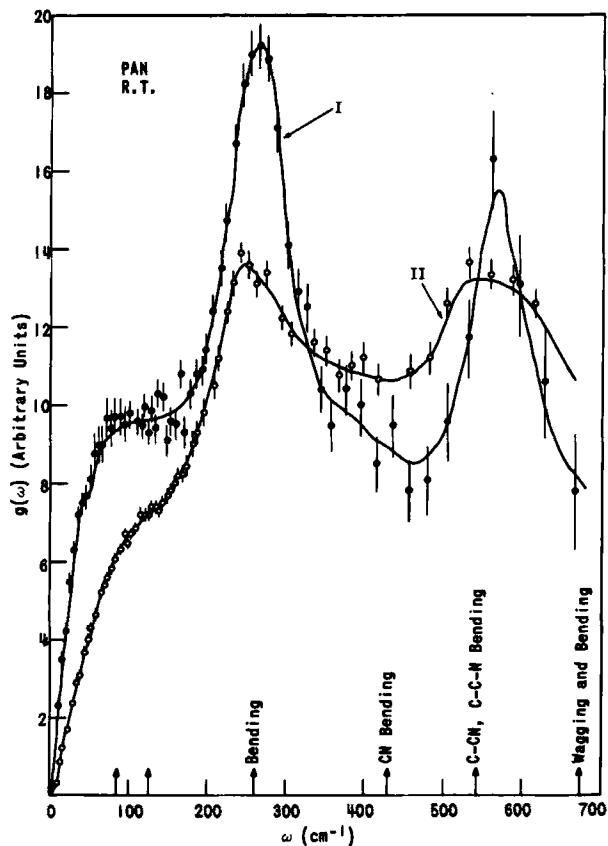
FIG. 11. Frequency distribution of the two samples of polyacrylonitrile derived as discussed in the text. The observed infrared frequencies are indicated together with their assignment.

expected to be most sensitive to chain order and would be the first to be broadened upon disordering of the chain. The differences in the neutron spectra of the two samples are striking. The two bands due to the optical modes are sharpened and the low-energy shoulder is better defined in sample I than in sample II. The relatively high degree of order observed in sample I reflects polymerization directly to a powder without passing through a solution or melt. The fact that the neutron spectrum of sample II becomes similar to that of sample I after a temperature cycling up to 150°C

indicates the existence of chain ordering, which increases irreversibly as the temperature is raised through the transitions. This chain ordering, which has not been suspected in the X-ray studies, may be a consequence of the better packing of the chains. Since no change in tacticity is expected to take place with increasing temperature, this ordering along the chain probably corresponds to an increase in length of the segments of the chain in a transplanar configuration.

Polyoxymethylene

The molecule of polyoxymethylene (POM) takes a helical conformation and contains nine monomer units (CH_2O) per identity period (19). Infrared and Raman spectra of this polymer have been obtained by several investigators (20), the lowest reported vibrational frequency being 235 cm^{-1}. Normal coordinate calculations have been performed in several of these works to make the band assignments. Several fundamental vibrations of the isolated chain are expected to occur below 200 cm^{-1}.

The neutron spectrum of a commercial sample of POM[*] in powder form was obtained at room temperature. The frequency distribution derived from this measurement is shown in Fig. 12(a). The structure below 200 cm^{-1} is due to the acoustic modes of the chains, which are optically inactive. The three lowest vibrational frequencies corresponding to optical modes which have been observed by infrared are approximately 237, 483, and 634 cm^{-1} (see Table 4).

To attempt an assignment of the bands observed in the neutron spectrum, additional measurements were obtained from an oriented sample of POM.[*] In this case, the momentum transfer $\bar{K}$ of the scattered neutron was placed alternatively parallel and perpendicular to the chain axis. The resulting frequency distributions reflect, as was shown in the case of oriented polyethylene, vibrations in which hydrogen atoms move along or transverse to the chain axis. The two frequency distributions obtained for POM are shown in Fig. 12(b) and (c). The peaks at 403 and 180 cm^{-1} correspond to longitudinal motions. Their intensity decreases appreciably when $\bar{K}$ is perpendicular to the direction of the chain axis. A

---

[*] The sample of POM was provided by Dr. H. Starkweather from E. I. du Pont de Nemours & Company.
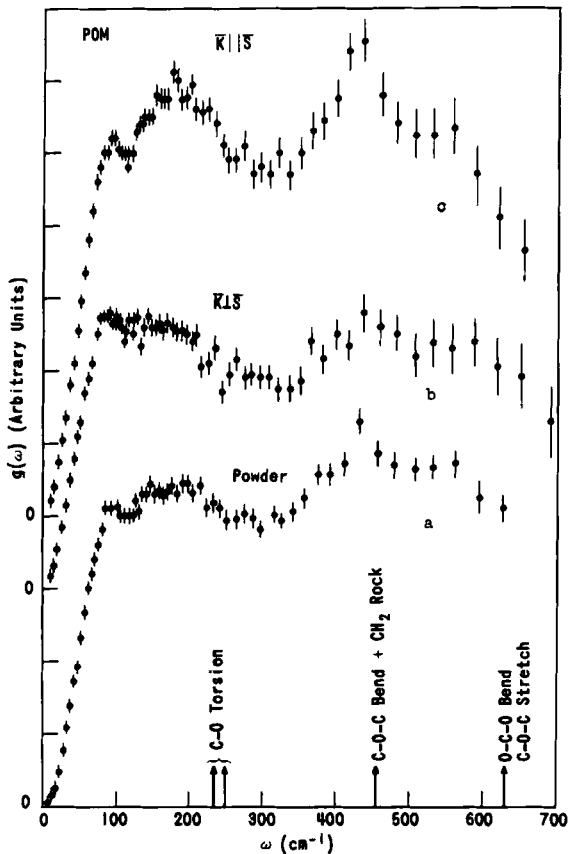
FIG. 12. (a) Frequency distribution of POM derived from the time-of-flight spectrum of neutrons scattered by a powder sample of the polymer at room temperature. (b) Frequency distribution of transverse modes. (c) Frequency distribution of longitudinal modes. The observed infrared frequencies are indicated in the lower portion of the figures together with their assignment.

normal coordinate calculation indicates that the peak at 180 cm^{-1} can be assigned to a mode analogous to the mode ν_5 (C—C—C bending and stretching) in polyethylene. The peak at 430 cm^{-1} is assigned to C—O—C bending mixed with CH$_2$ rocking. It may correspond to a peak at 480 cm^{-1} in the infrared spectrum. The peak around 80 cm^{-1} in the neutron spectrum is observed with both polarizations. It may correspond to a mode similar to the mode ν_9 (C—C torsion) in polyethylene. A shoulder is also observed

TABLE 4

Comparison of the Vibrational Frequencies in POM Observed by Infrared and Neutron Measurements with the Calculated Values[a]

Neutron	Infrared	Calc.	Assignment[b]
1045	1097	1118	$\nu_a(COC)(77) + r(CH_2)(19)$
	1091	1072	$\nu_a(COC)(70) - \delta(OCO)(26)$
844	903	922	$r(CH_2)(75) - \nu_a(COC)(21)$
	932	930	$\nu_s(COC)(74) + r(CH_2)(23)$
568	630	634	$\delta(OCO)(74) + \nu_a(COC)(20)$
470	455	483	$\delta(COC)(64) - r(CH_2)(28)$
288			
248	235	237	$\tau_a(96) + r(CH)(3)$
208			
180			
97			
80			
50		22	$\tau_s(56) - \tau_a(40)$

[a] The possible assignments are taken from Tadokoro et al. The frequencies are expressed in cm^{-1}.
[b] ν, stretching; ν, symmetric stretching; ν_a, antisymmetric stretching; τ, torsion; τ_s, symmetric torsion; τ_a, antisymmetric torsion; δ, bending; r, rocking.

in the neutron spectrum around 130 cm^{-1}. The infrared frequency at 235 cm^{-1} has been assigned to a torsional vibration. The neutron spectrum in that frequency region shows only a broad distribution which is not well resolved from the 180 cm^{-1} band. There is also evidence of some structure in the 500 to 600 cm^{-1} range which might correspond to infrared inactive frequencies.

These measurements provide a useful basis, in addition to the infrared results, for a calculation of the frequency distribution of the vibrations of a POM chain.

Acknowledgments

REFERENCES

1. G. J. Safford, H. R. Danner, H. Boutin, and M. Berger, *J. Chem. Phys.*, **40**, 1426 (1964).
2. H. R. Danner, G. J. Safford, H. Boutin, and M. Berger, *J. Chem. Phys.*, **40**, 1417 (1964).
3. J. S. King and J. L. Donovan, *Bull. Am. Phys. Soc.*, **9**, 623 (1964).
4. W. L. Whittemore, *Scattering of Neutrons by Polyethylene*, General Atomic Rept. GA-6456 (1965).
5. H. Boutin, H. Prask, S. F. Trevino, and H. R. Danner, *Inelastic Scattering of Neutrons*, IAEA, Vienna, **II**, 407 (1965).
6. W. Myers, J. L. Donovan, and J. S. King, *J. Chem. Phys.*, **42**, 4299 (1965).
7. W. Myers, G. C. Summerfield, and J. S. King, *J. Chem. Phys.*, **44**, 184 (1966).
8. M. Tasumi and T. Shimanouchi, *J. Chem. Phys.*, **43**, 1245 (1965); M. Tasumi, T. Shimanouchi, and T. Miyazawa, *J. Mol. Spectr.*, **9**, 261 (1962); T. P. Lin and J. L. Koenig, *J. Mol. Spectr.*, **9**, 228 (1962); M. Tasumi and T. Shimanouchi, *J. Chem. Phys.*, **43**, 1245 (1965).
9. T. Kitagawa and T. Miyazawa, *Rept. Progr. Polymer Phys. Japan*, **7**, 53 (1965).
10. A. Sjölander, *Arkiv Fysik*, **14**, 315 (1958).
11. L. V. Tarasov, *Soviet Phys.-Solid State (English Transl.)*, **3**, 1039 (1961).
12. S. Krimm, C. Y. Liang, and G. B. B. M. Sutherland, *J. Chem. Phys.*, **25**, 543, 549 (1956).
13. B. Wunderlich, *J. Chem. Phys.*, **37**, 1203 (1962).
14. H. Tadokoro, Y. Chatani, T. Yoshihara, S. Tahara, and S. Murahashi, *Makromol. Chem.*, **73**, 109 (1964).
15. C. R. Bohn, J. R. Schaefgen, and W. O. Statton, *J. Polymer Sci.*, **55**, 531 (1961).
16. R. D. Andrews and R. M. Kimmel, *J. Appl. Phys.*, **35**, 3194 (1964); *Polymer Letters*, **3**, 167 (1965).
17. C. Y. Liang and S. Krimm, *J. Polymer Sci.*, **31**, 513 (1958).
18. R. Yamadera, H. Tadokoro, and S. Murahashi, *J. Chem. Phys.*, **41**, 1233 (1964); T. Miyazawa, *J. Chem. Phys.*, **35**, 693 (1961).
19. H. Tadokoro, T. Yasumoto, S. Murahashi, and I. Nitta, *J. Polymer Sci.*, **44**, 266 (1960).
20. H. Tadokoro, M. Kobayashi, Y. Kawaguchi, A. Kobayashi, and S. Murahashi, *J. Chem. Phys.*, **38**, 703 (1963) and references therein.

Zusammenfassung

Die Energieverteilung eines mono-energetischen Neutronenstrahls lässt nach einem einzigen Streuungsvorgang Schlüsse zu auf die Molekularbewegungen eines Polymeren im Bereich von 800 bis 30 cm⁻¹. In Polyethylen (Marlex 6050) wurden im Neutronenspektrum im Bereich von 200 bis 600 cm⁻¹ mehrere Banden beobachtet. Die diesen Banden

entsprechenden Frequenzen stimmen gut mit vorausgesagten Werten-
überein die aus den Dispersion Beziehungen der Skelettschwingungen
(bending und stretching) unter Berücksichtigung von zwischen Ketten
auftretenden Kräften berechnet wurden. Im Falle einer orientierten Probe
eines polymeren Materials kann ein Polarisationseffekt dadurch erhalten
werden, indem die Momentübertragung der Neutronen $\bar{K}$ parallel oder
senkrecht zur Richtung der Ketten $\bar{S}$ gelegt wird. Dadurch können trans-
versale und longitudinale Schwingungen identifiziert werden. Dieser
Effekt wurde in Polyethylen und Polyoxymethylen untersucht. Die aus
den Neutronendaten unter bestimmten Näherungen abgeleitete Frequenz-
verteilung der Phononen wurden auch in Proben von Polyoxymethylen,
Polyacrylnitril und Polyäthylenglycol erhalten. Diese Ergebnisse werden
mit ben beobachteten und berechneten IR Frequenzen verglichen.

Résumé

La distribution d'énergie d'in faisceau incident monoénergétique de
neutrons fournit après une seule dispersion des reinsegnements con-
cernant les mobilités moléculaires d'un polymère dans la region de 800
à 30 cm^{-1}. On a observé plusieurs maxima dans le spectre des neutrons
entre 200 et 600 cm^{-1} pour le polyethylène (Marlex). Les fréquences qui
corrèspondent à ces maxima sont en bon accord avec les valeurs calculées
à l'aide des relations de dispersions des modes de vibrations du squelette
(flexion et allongement), tenant compte des forces entre les chaînes. Dans
les cas d'un échantillon orienté du polymère, on peut obtenir un effet
polarisant en mettant le moment de transfert $\bar{K}$ du neutron parallèlement
ou perpendiculiérement à la direction $\bar{S}$ de la chaîne. Cela permet l'identi-
fication des modes de vibration transversales et longitudinales. On a
étudié cet effet dans le cas de polyéthylène et polyoxyméthylène. On a
aussi obtenu la distribution de fréquence des phonones, par derivation des
données du neutron sous certains approximations, pour des echantillons de
polyoxyméthylène, de polyacrylonitrile et de polyéthylène glycol. On a
comparé ces résultats avec les fréquences observées dans l'infrarouge et les
fréquences calculées.